FN-286
2562.000

Fermilab

A TWO-DIMENSIONAL READOUT DRIFT CHAMBER WITH PRINTED CIRCUIT DELAY LINES

M. Atac, R. Bosshard[†], Y. Kang

Fermi National Accelerator Laboratory

P. O. Box 500

Batavia, Illinois 60510

[†]Laboratory Accelerateur Lineaire, Orsay, France

December, 1975

ABSTRACT

A two-dimensional readout drift chamber with printed circuit zig-zag delay lines has been developed. Track position accuracies of 3-5 mm from the delay line and 80-100μ from the electron drift time have been obtained.

A TWO-DIMENSIONAL READOUT DRIFT CHAMBER WITH PRINTED CIRCUIT DELAY LINES

Introduction

Obtaining two-dimensional coordinate measurements of a track from a proportional or a drift chamber cell is desirable especially for high multiplicity experiments. Having a pair of correlated coordinates for every track would reduce multi-track ambiguities and consequently decrease computing costs. Here we offer an elegant and practical delay line readout which can be conveniently constructed in a parallel foil drift chamber (PFDC).[1,2] In this case, printed circuit tape delay lines (zig-zag lines) replacing the parallel drift foil electrodes provide a second coordinate for a track in a cell. The second coordinate is measured through the zig-zag delay lines by induced pulses. On the other hand, the first coordinate is obtained from the drift time of the electrons produced by ionization during the passage of a charged particle with an accuracy of 80-100μ.[1,2] This type of delay line readout eases the difficulties in measuring a longitudinal track coordinate in a cylindrical geometry.

In the following, we will describe a prototype PFDC of 50 cm x 50 cm active area (25 cells) in which two of the aluminum foils were replaced with a pair of printed circuit thin foil delay lines. The results show that a track position accuracy σ of 3 to 5 mm can be obtained along the delay line.

Chamber Construction

Figure 1 shows a simplified perspective view of the chamber together with a cross sectional view. In the perspective view, the dimensions shown are not to scale for clarity and simplicity.

The dimensions of the cells are indicated in the cross sectional view. The chamber has a sensitive area of 50 cm x 50 cm and it contains 25 drift cells. The signal wires were soldered in positions within 5μ accuracy and the delay lines were glued with Eastman 910 to the positioning blocks within 25μ accuracy. We will not give every detail of PFDC construction since some of the details are given in the earlier reports.

The Delay Lines

The delay line has two characteristic features. It provides a uniform electric field and it senses the induced signal. Consequently, results in delay time measurements, at its ends from which the track positions along the sense wire, are obtained. Desirable characteristics of such a delay line are:

a) High characteristic impedance Z to achieve primarily good signal to noise ratio which is proportional to $Z^{\frac{1}{2}}$.

b) Good coupling efficiency η (see page 3).

c) Long delay time, τ, per unit length.

d) A reasonable balance among signal losses due to d.c. resistance, skin effect, dispersion and the thickness of the conductive material (multiple coulomb scattering).

Most of the above objectives are achieved by maintaining a flat geometry by using a printed circuit technique. This is

illustrated in Figure 2a. The delay lines are photo-etched on both sides of Copper-cladded (25μ thick) Mylar (65μ thick) strips. The rest of the dimensions are given with the figure. The conductive planes on a strip are shifted by a half period in order to boost the inductance L while maintaining a constant capacitance C, thus simultaneously increasing impedance Z and the delay time τ.

Figure 2b shows how this takes place. The currents I in the two conductors (in the region where they overlap) are in the same direction thereby enhancing the mutual inductance. From theory, the inductance of an iterative loop can be seen to be four times the inductance of a single loop. For the lines considered here, the single loop inductance is three times the inductance of the strip (non-shifted zig-zag) of the same length. As a result, we get a factor of 12 in inductance, thus an increase of about a factor of 3.5 in Z and τ. Some details on the delay lines are given in Reference 3.

The coupling efficiency η of the delay line looking toward the anode wire is related by the difference between the induced charge on the forward zig-zag plane q_f and that seen by the backward zig-zag plane q_b. Since these charges are proportional to the capacitances c_f and c_b, we define η to be:

$$\eta = \frac{C_f - C_b}{C_f + C_b} \qquad (1)$$

The η is also dependent on the ratio of the width W over the spacing S of the delay line. To improve η the ratio W/S of the

forward plane can be increased relative to that of the backward plane. In this way, coupling efficiency of 80% has been achieved without losing much of the properties of the line.

The skin effect and the d.c. resistance are mainly the limiting factors in choosing a practical length for a delay line. To see the characteristic skin effect, we shall take the value of the rise time for a step function to rise to its 50% amplitude as given by the theory of long cables (Reference 5),

$$t_{50} = \frac{\rho\mu}{4Z^2}\left(\frac{\ell_o}{W}\right)^2 \qquad (2)$$

where ρ is the resistivity, μ is the permeability, Z is the characteristic impedance, W is the width, and the ℓ_o is the total length of the conductor in one plane. Four times this value is taken in the case of the delay line. For copper, we obtain the following practical formula in MKS units:

$$t_{50} \simeq \frac{2.10^{-4}}{Z^2}\left(\frac{\ell}{W}\right)^2 \qquad (3)$$

We see from this expression that it is important to achieve a high impedance Z for our 50 cm long delay line. We get $t_{50} \simeq 3.6$ nsec from the conductor of 250μ width and $\ell_o \simeq 8$ m with an impedance of 75Ω and with a pulse attenuation factor of 20%.

Tests with X-Ray Source

Well-collimated 5.9 keV x-rays of Fe^{55} were used for the tests to measure some of the characteristics of the chamber and the delay lines, while $Ar/C_2H_2/CH_4$ gas mixture is flowed through

the chamber. The gas is flow mixed with flow ratios of 22% C_2H_2 and 78% of Ar-CH_4 (90% Ar - 10% CH_4 pre-mixed). A gas gain of 5×10^5 is achieved with this gas at a voltage of 2.3 kV applied to the chamber cells operating in the proportional region. Figure 3 shows induced signals which are integrated over 5μsec obtained from the delay line with external triggers from the anode pulses. The 5.9 keV x-ray line and the escape line are clearly seen in the figure. An inverting charge amplifier is used to obtain the picture. The induced signal on the line is about 20% of the anode signal. Figure 4 shows the current pulses which are obtained differentially from the delay lines using the current amplifier shown in Figure 5. Since the pulses are quite small, the success of the delay line operation depends on the signal to noise ratio. Care is taken to reduce the noise with this amplifier design. These current pulses are about 6% of the full current signals obtained from the anode wire.

The collimated source was moved in steps of 2 cm along the drift chamber cell. Figure 6 shows some delay time spectra obtained from the difference time measurements which are measured by a time-to-amplitude converter and stored in a pulse height analyzer. Figure 7 shows a good linear relation between the position of the source and the mean delay time difference. When the source is displaced 1 cm in the difference measurement this corresponds to 4.4 nsec, thus providing 2.2 nsec/cm delay in the transmission of the induced pulses in both directions of the delay line. The standard deviations from the mean values in measurements of the source positions along the line are determined

to be σ = 3 mm in the entire range shown in the figure.

Tests at the Beam Line

Further tests were carried out at the M6 West beam line of the Meson Laboratory using 100 GeV/c pion beam. The beam was defined by a pair of plastic scintillators of 5 mm x 10 mm size (5 mm width is in the direction of the delay line). The delay times were measured by a pair of time digitizer circuits in CAMAC system as the chamber moved relative to the beam. The trigger pulse obtained from the anode wire started the TDC's. The data was stored in tapes of a PDP-11 computer and analyzed off-line. Figure 8 shows two typical superimposed current pulses obtained from one end of the delay line. The time structure is due to successive gas multiplication of electrons as they reach the anode wire. This geometrical effect is one of the limiting factors of multiple track resolution of a drift chamber cell. The width of the time structure is varied between 100 to 150 nsec for our geometry. Figure 9 shows a good linear relation between the track position and the delay time. A position accuracy of σ = 5 mm was obtained in the entire range.

The delay line system efficiency for obtaining a signal above the noise level was measured to be about 60% for the pion beam. We believe that this can be improved with an asymmetric construction of the chamber as indicated in Figure 10 by increasing the capacitance between the signal wires and the delay line.

REFERENCES

1. M. Atac and W. E. Taylor, Nucl. Instr. and Meth. 120 (1974), 147-151.

2. M. Atac and C. Ankenbrandt, IEEE Transactions on Nuclear Science, Vol. NS-22, No. 1 (1975), 306.

3. R. Bosshard, R. L. Chase, J. Fisher, and V. Radeka, Brookhaven National Laboratory preprint.

4. G. Amsel and R. Bosshard, Rev. of Scientific Instr., Vol. 41, No. 4 (1970), 503-514.

5. R. L. Wigington and N. S. Nahman, PIRE 45 (1957), 166.

FIGURE CAPTIONS

Figure 1.. A simplified perspective view and a cross section view of the chamber.

Figure 2. a) A descriptive view of the delay line strip.
b) Schematic view of the current loops.

Figure 3. Induced pulses at one end of the delay line obtained from an Fe^{55} source. The 5.9 keV x-ray line and the escape line are seen in the picture. Pulses are integrated over 5μsec.

Figure 4. The current pulses obtained from the delay line using Fe^{55} source and the amplifier shown in Figure 5. The scales are 20 nsec per division and 0.1v per division.

Figure 5. The circuit diagram of the current amplifier.

Figure 6. Delay time spectra obtained from the pulse height analyzer using a time-to-amplitude converter. The Fe^{55} source is moved in steps of 2 cm along the delay line.

Figure 7. Source position to delay time relation.

Figure 8. A picture of current pulse time structure resulted from 100 GeV/c pion beam tracks. Horizontal scale is 50 nsec per division.

Figure 9. Track position to delay time relation.

Figure 10. A schematic view of the asymmetric construction of the drift chamber to improve the coupling efficiency of the delay line.

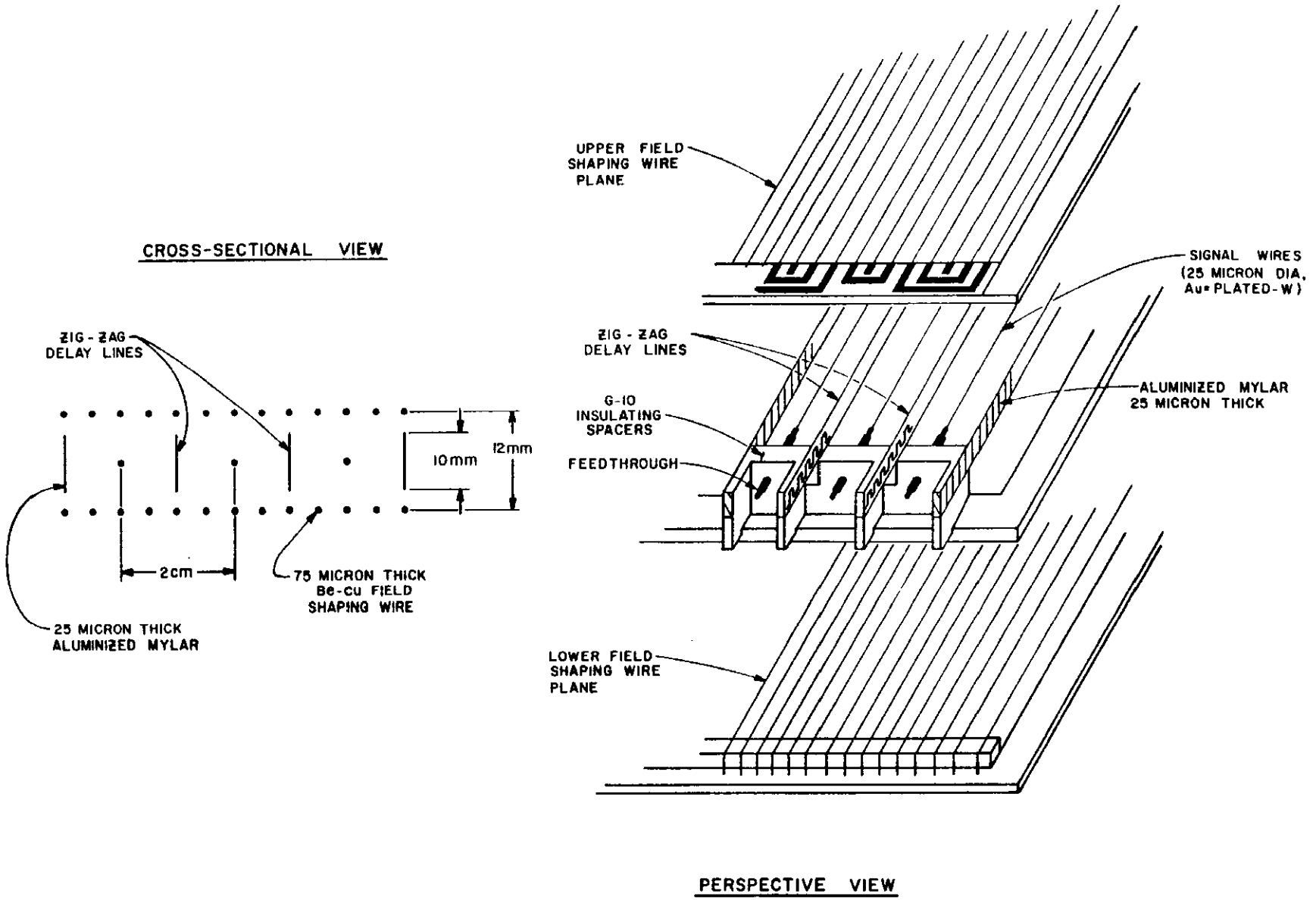
CROSS-SECTIONAL VIEW
ZIG - ZAG DELAY LINES
10mm
12mm
2cm
75 MICRON THICK Be-Cu FIELD SHAPING WIRE
25 MICRON THICK ALUMINIZED MYLAR
UPPER FIELD SHAPING WIRE PLANE
SIGNAL WIRES (25 MICRON DIA, Au-PLATED-W)
ZIG - ZAG DELAY LINES
ALUMINIZED MYLAR 25 MICRON THICK
G-10 INSULATING SPACERS
FEEDTHROUGH
LOWER FIELD SHAPING WIRE PLANE
PERSPECTIVE VIEW

FIG. 1

FN-286

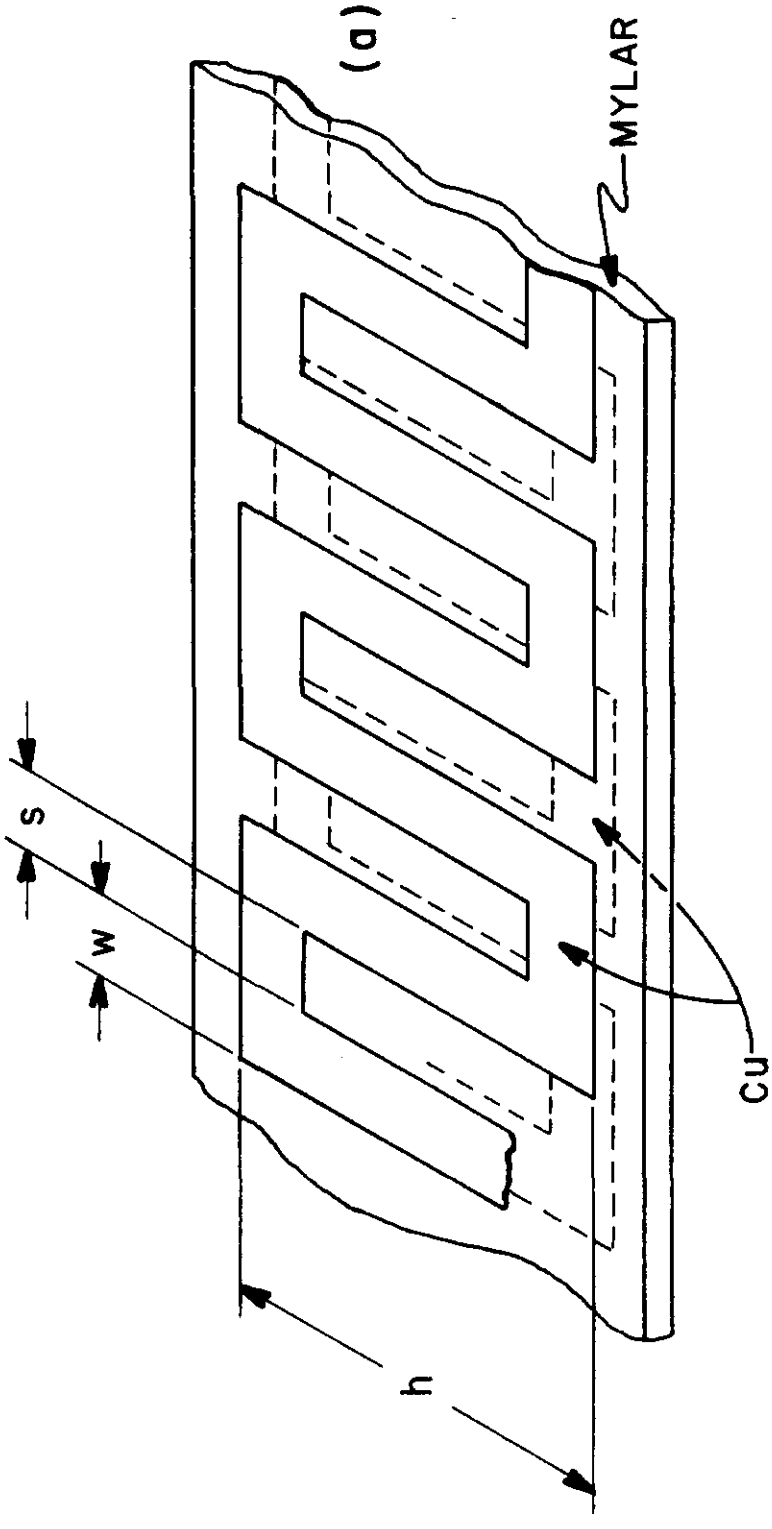

FIG. 2

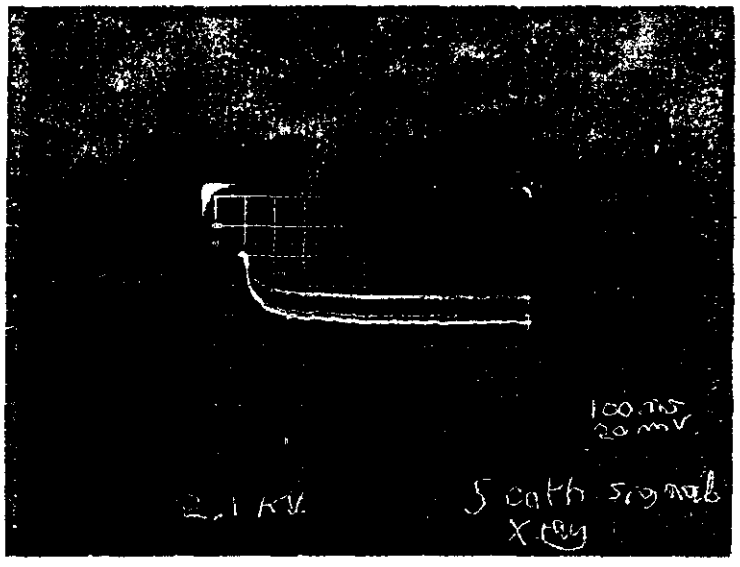

FIG. 3

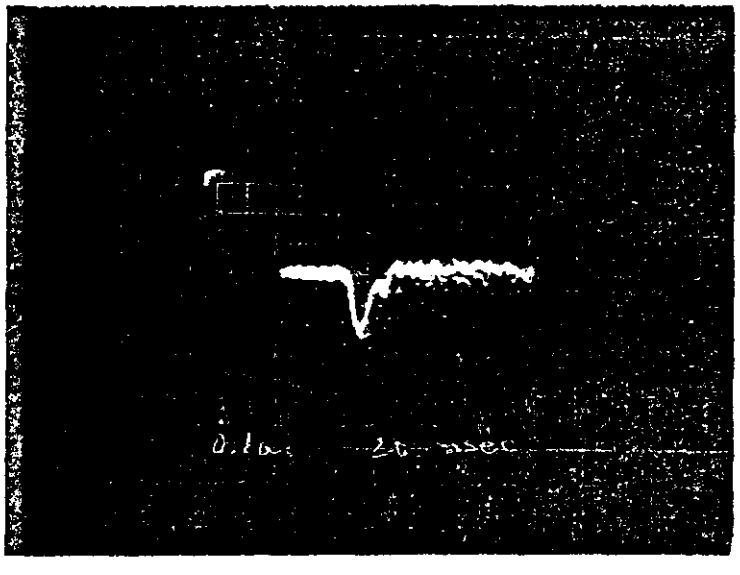

FIG. 4

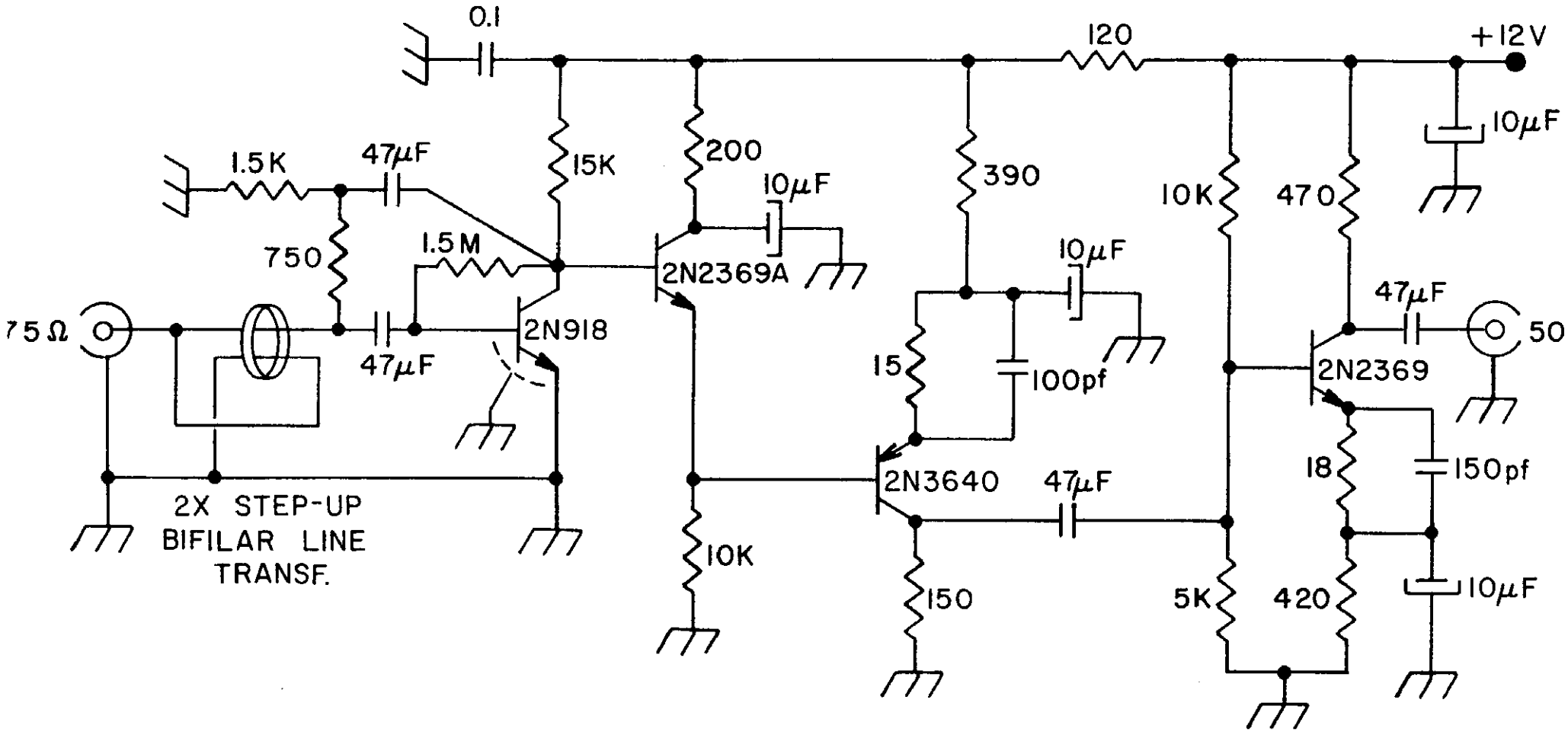

AMPLIFIER CIRCUIT

FN-286

FIG. 5

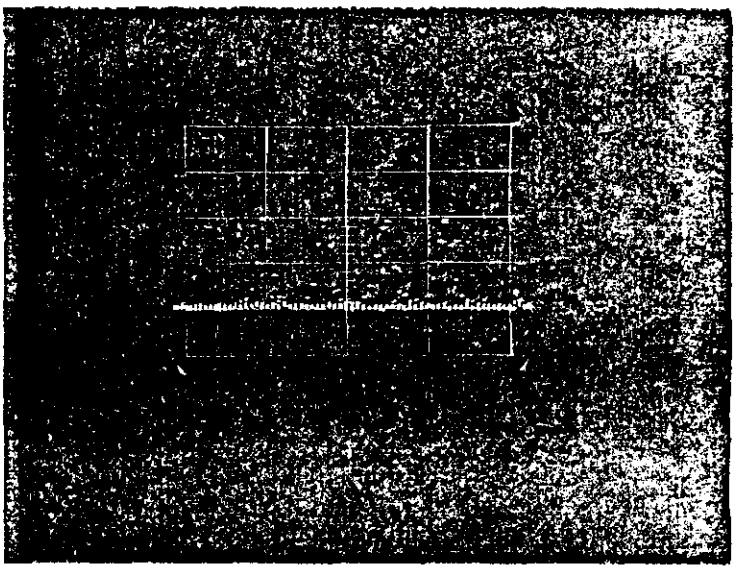

FIG. 6

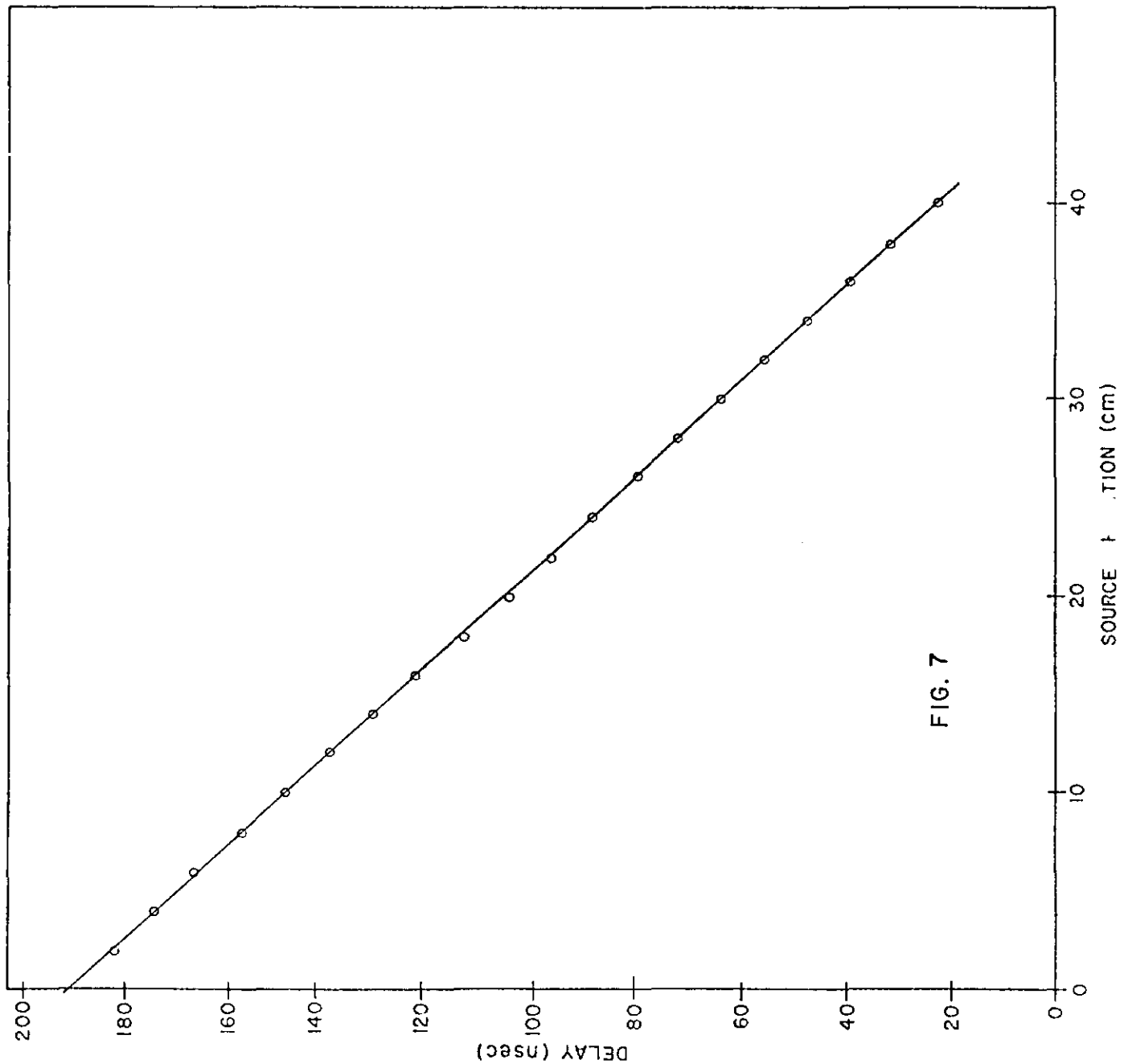
DELAY (nsec)
200
180
160
140
120
100
80
60
40
20
0
0
10
20
30
40
SOURCE TION (cm)

FIG. 7

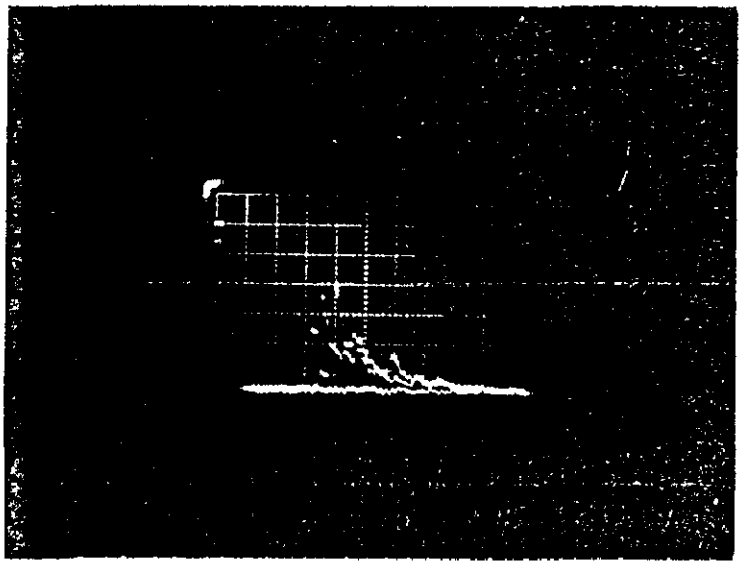

FIG. 8

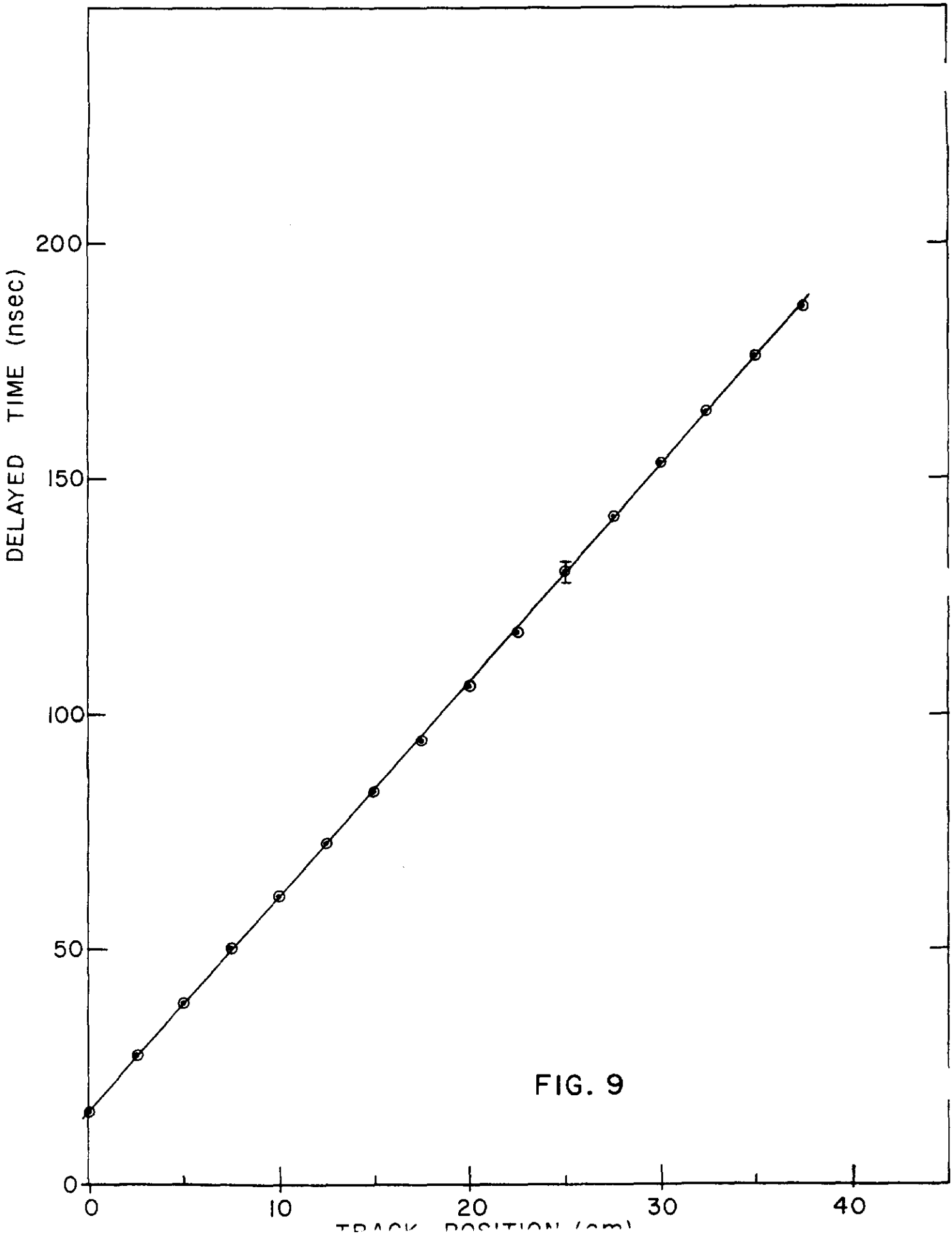

FIG. 9

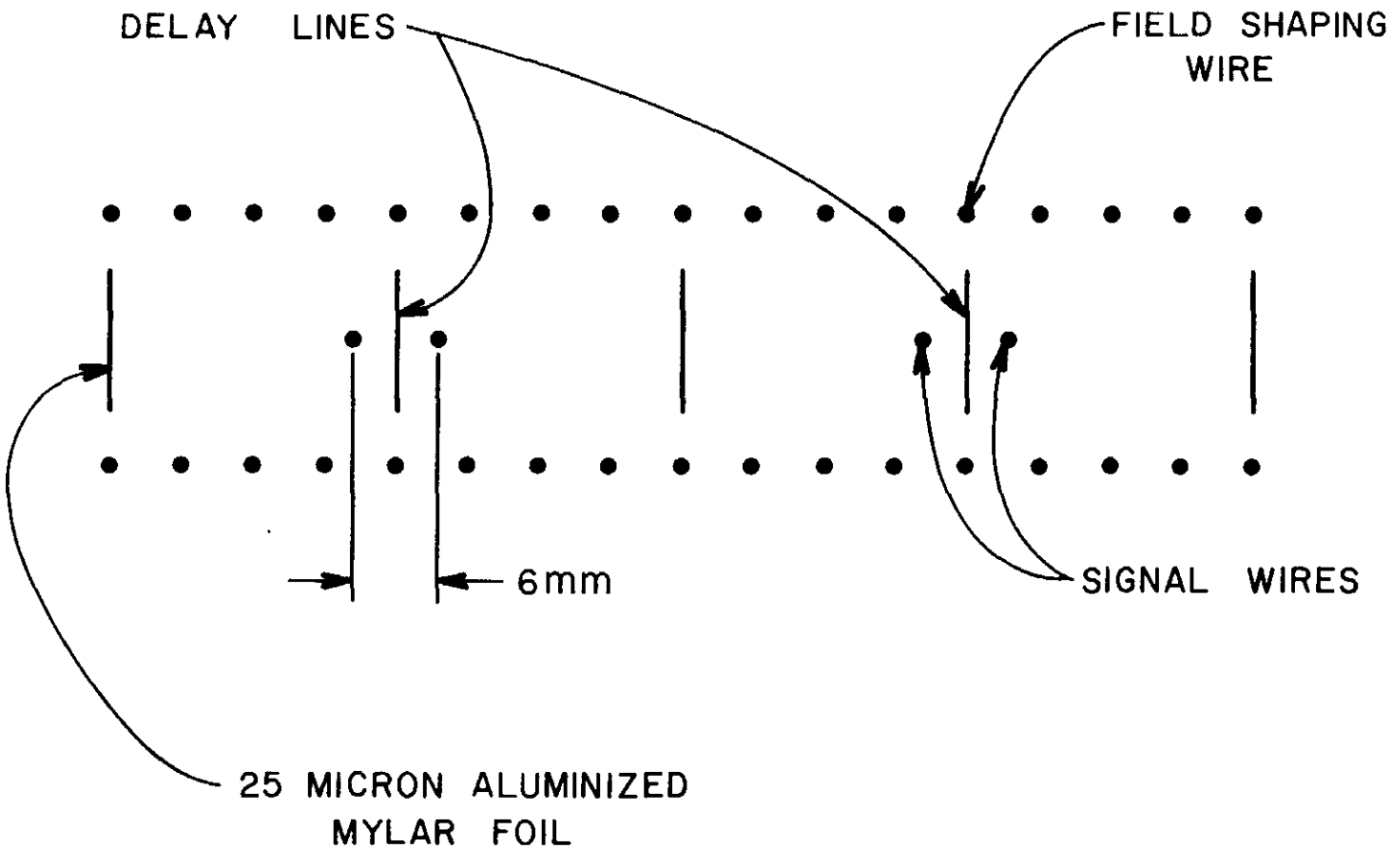
DELAY LINES
FIELD SHAPING WIRE
6mm
SIGNAL WIRES
25 MICRON ALUMINIZED MYLAR FOIL

FIG. 10

FN-286